PCCP

Vibrational Circular Dichroism towards Asymmetric Catalysis: Chiral Induction in Substrates Coordinated with Copper(II) Ions

Journal:	*Physical Chemistry Chemical Physics*
Manuscript ID	CP-ART-09-2020-004827.R1
Article Type:	Paper
Date Submitted by the Author:	14-Oct-2020
Complete List of Authors:	Sato, Hisako; Ehime University, Department of Chemistry Takimoto, Kazuyoshi; Ehime University, Yoshida, Jun; Kitasato University, chemistry Yamagishi, Akihiko; Toho University Omori Medical Center

ARTICLE

Vibrational Circular Dichroism towards Asymmetric Catalysis: Chiral Induction in Substrates Coordinated with Copper(II) Ions

Hisako Sato, [a*] Kazuyoshi Takimoto, [a] Jun Yoshida[b] and Akihiko Yamagishi[c]

Received 00th January 20xx
Accepted 00th January 20xx

DOI: 10.1039/x0xx00000x

Cu(II) complexes containing *RR*- or *SS*-2,2'-isopropylidene-bis(4-phenyl-2-oxazoline) (denoted as [Cu(*RR*- or *SS*-oxa)]$^{2+}$) are known to catalyse many asymmetric organic reactions. Herein, the source of enantioselectivity was investigated by vibrational circular dichroism (VCD) spectroscopy. An achiral β-diketonato ligand (denoted as LH), such as 1-phenyl-1,3-butanedione and dibenzoylmethane, was added to form [Cu(*RR*- or *SS*-oxa)L]$^{+}$. Clear VCD peaks were obtained from a $CDCl_3$ solution of [Cu(*RR*- or *SS*-oxa)]$^{2+}$ or [Cu(*RR*- or *SS*-oxa)L]$^{+}$ at 1000–1800 cm^{-1}. It is to be noted that when LH was coordinated, a new VCD peak appeared at ~1380 cm^{-1}, which was assigned to the C–O asymmetric stretching vibration of L^{-}. Theoretical simulation helped rationalise the results in terms of the transformation of coordinated L^{-} into a twisted chiral form. The extent of steric control within the coordination sphere was demonstrated, revealing the first step for enantioselectivity during catalysis.

Introduction

Enantioselective reactions catalysed using metal complexes are commonly performed to obtain enantiopure compounds in both homogenous and heterogeneous systems.[1-15] Copper(II) complexes are used due to their excellent Lewis acidity. Evans *et al.* reported the synthesis of chiral bis(oxazoline)copper(II) complexes with catalytic activity for a wide range of reactions, including carbocyclic, Diels-Alder, aldol addition, Michael addition, and enol amination reactions.[2,13] In heterogeneous catalysis, the Cu(II) complexes could be immobilized on inorganic supports, such as layered clay minerals,[8] with similar effectiveness as in a solution.[2]

The high enantioselectivity exhibited by these Cu(II) complexes prompted us to examine the origin of chiral discrimination. Vibrational circular dichroism (VCD) spectroscopy was employed to reveal the steric control within a coordination sphere.[16,17] The method is powerful for clarifying the details of stereoselective intermolecular interactions in solutions.[18-28] Recently, Merten *et al.* applied VCD to asymmetric catalysts to examine the interactions between a catalyst and a substrate, where a chiral thiourea catalyst formed a hydrogen bond with the substrate.[20]

In this study, VCD methods were applied on [Cu(*RR*- or *SS*-2,2'-isopropylidene-bis(4-phenyl-2-oxazoline)]$^{2+}$ (denoted as [Cu(*RR*- or *SS*-oxa)]$^{2+}$; Chart 1(a) and (b) for *RR*- and *SS*-ligands, respectively). As a model reaction intermediate, an achiral β-diketone (denoted as LH), such as 1-phenyl-1, 3- butanedione (bzacH) and dibenzoylmethane (dbmH; Chart 1(c) and (d), respectively), was coordinated to form [Cu(*RR*- or *SS*-oxa)L]$^{+}$. A hexagonal chelated ring was formed with the Cu(II) ion. Such ring formation was suggested as an intermediate in the case of a di-carbonyl substrate (Chart 1(e)). The effect of the conformation of coordinated L^{-} on the steric control within the coordination sphere was examined.

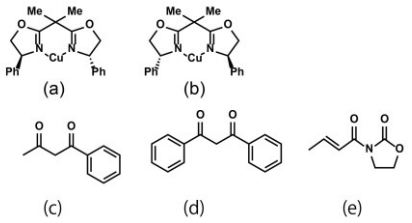

Chart 1. Molecular structures of (a) [Cu(*RR*-oxa)], (b) [Cu(*SS*-oxa)], (c) bzacH, (d) dbmH, and (e) 3-(*E*)-2-butenoyl-2-oxazolidinone (denoted as ***S***)

Results and Discussion

Preparation of Cu(II) complexes: [Cu(*RR*- or *SS*-oxa)]$^{2+}$ was prepared by mixing equimolar amounts of copper(II) trifluoromethanesulfonate (denoted as [Cu(TFMS)$_2$]) and *RR*- or *SS*-2,2'-isopropylidene-bis(4-phenyl-2-oxazoline) (denoted as *RR*- or *SS*-oxa, respectively) in methanol. The progress of a reaction was monitored by the change of a UV-vis spectrum (see ESI†). [Cu(*RR*- or *SS*-oxa)L]$^{2+}$ (L^{-} = achiral β-diketonato ligand) was prepared by adding the equimolar amounts of LH

[a] Graduate School of Science and Engineering, Ehime University, Matsuyama 790-8577, Japan, sato.hisako.my@ehime-u.ac.jp
[b] Department of Chemistry, Kitasato University, Sagamihara 252-0329, Japan
[c] School of Medicine, Toho University, Ota-ku, Tokyo 143-8540, Japan

†Electronic Supplementary Information (ESI) available: UV-vis spectra of [Cu(RR-oxa)]$^{2+}$; HPLC chromatograms of [Cu(SS-oxa)]$^{2+}$ and[Cu(SS-oxa)L]$^{+}$; Mass spectra of [Cu(SS-oxa)]$^{2+}$and[Cu(SS-oxa)L]$^{+}$; Calculated VCD and IR spectra of [Cu(SS-oxa)]$^{2+}$, [Cu(SS-oxa)](TFMS)$^{+}$and [Cu(SS-oxa)](TFMS)$_2$ for the optimized structures; Calculated VCD and IR spectra of [Cu(SS-oxa)(bzac)]$^{+}$ for the optimized structure; Assignment of the main peaks in the experimental VCD spectra, See DOI: 10.1039/x0xx00000x

(LH = bzacH and dbmH; Chart 1 (c) and (d), respectively) to a methanol solution of [Cu(*RR*- or *SS*-oxa)] $(TFMS)_2$. These ligands were chosen as the model substrates because of the high chelating capability for Cu(II). The methanol solutions containing these complexes were analysed by high-performance liquid chromatography (HPLC), showing a single peak in the chromatogram (ESI^+). Each peak was collected and analysed by mass spectrometry, which identified the compounds as [Cu(*SS*-oxa)](TFMS)$^+$ ($C_{22}H_{22}CuN_2O_5F_3S$), [Cu(*SS*-oxa)(bzac)]$^+$ ($C_{31}H_{31}CuN_2O_4$), and [Cu(SS-oxa)(dbm)]$^+$ ($C_{36}H_{33}CuN_2O_4$), respectively (see $ESI^†$).

Changes in the electronic circular dichroism (ECD) spectrum was monitored upon bzacH or dbmH addition to a methanol solution of [Cu(*RR*- or *SS*-oxa)](TFMS)$_2$, as shown in Figure 1. A novel peak appeared at approximately 325 nm with a negative or positive sign for *RR*- or *SS*-oxa, respectively. The position of the peak corresponded to the $\pi \text{---} > \pi*$ transition of bzac$^-$ or dbm$^-$. Thus, the observed peak was regarded as ECD induced in L$^-$. Because the free LH was achiral, the ECD results confirmed the binding of LH to the chiral Cu(II) complexes as shown below:

[Cu(*RR*- or *SS*-oxa)]$^{2+}$ + LH
→ [Cu(*RR*- or *SS*-oxa)L]$^+$ + H$^+$

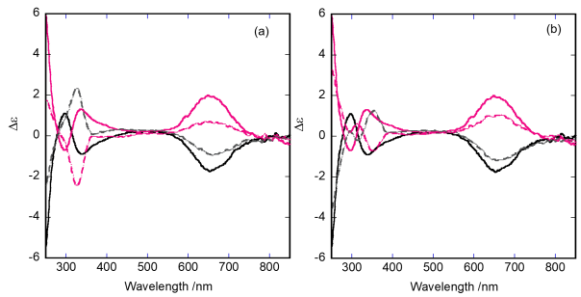

Figure 1. ECD spectra of the methanol solutions of [Cu(*RR*-oxa)](TFMS)$_2$ (solid black) and [Cu(*SS*-oxa)](TFMS)$_2$ (solid red). Equimolar amounts of LH were added to each solution; LH = bzacH (a) and dbmH (b). Dotted black and red lines represent the resultant ECD spectra of [Cu(*RR*-oxa)L]$^+$ and [Cu(*SS*-oxa)L]$^+$, respectively. The new peaks appearing at approximately 325 nm were assigned to the electronic dichroism induced in the coordinated L$^-$.

VCD spectra of [Cu(*RR*- or *SS*-oxa)]$^{2+}$ and [Cu(*RR*- or *SS*-oxa)L]$^+$ in solution: Figure 2(a) shows the IR and VCD spectra of [Cu(*RR*- or *SS*-oxa)] $(TFMS)_2$ in $CDCl_3$. The mirror image relation was maintained between the *RR* and *SS* ligands. The main peaks were numbered in the order of decreasing wavenumber. Each VCD peak could be paired with a corresponding IR peak at the same wavenumber. Peaks **1** and **2** were assigned as in-phase (symmetric) and out-of-phase (asymmetric) stretching vibrations of C–N bonds in the coordinated oxa ligand, respectively. Peaks **3** and **4** were assigned to the C-C-C stretching vibrations of phenyl groups, while the couplet peaks **5** and **6** at approximately 1500 cm^{-1} were assigned to the C-H bending of phenyl groups and CH_3 scissoring of methyl groups, respectively. The IR bands at approximately 1200–1300 cm^{-1} indicated by no. **8** and **9** were assigned to the overlap of S-O, S-C stretching and the C-F stretching vibrations of TFMS anions and the bending vibration of C-H at the chiral centre of an oxa ligand. The IR peaks indicated by nos. **10** and **11** were assigned to the stretching vibrations of the S-O and C-F bonds in the anion.[28] None of these peaks showed VCD activity, indicating that the anion remained achiral.

Figure 2(b) shows the IR and VCD spectra of [Cu(*RR*- or *SS*-oxa)(bzac)](TFMS) in $CDCl_3$. The mirror image relation was maintained between the *RR* and *SS* ligands. When the spectra were compared with those of [Cu(*RR*- or *SS*-oxa)](TFMS)$_2$, new IR peaks corresponding to **a–d** could be assigned to the coordinated bzac$^-$. Notably, an intense new VCD peak appeared at approximately 1378 cm^{-1} (indicated by **c**), assigned to the stretching vibrations of the C-O skeleton of bzac$^-$. This indicated that bzac$^-$ transformed and became chiral upon coordination with Cu(II). The details of the structural transformation accompanied by VCD peak generation will be discussed later with the assistance of theoretical simulation. However, it should be emphasised that the appearance of a new peak in the ECD spectrum of [Cu(*RR*- or *SS*-oxa)(bzac)]$^+$ (Figure 1) did not necessarily indicate that bzac$^-$ formed a chiral structure. The induction of an ECD peak can occur from electronic causes alone without accompanying structural changes.[29]

Similar results were obtained for the VCD and IR spectra of [Cu(*RR*- or *SS*-oxa)(dbm)](TFMS) (Figure 2(c)). The new VCD peaks **a–d** assigned to the coordinated dbm appeared, indicating that dbm$^-$ became chiral upon coordination. Thus, chiral structure adoption occurred even for a symmetric β-diketonato ligand. The detailed VCD spectral analyses are provided in the next section with the assistance of theoretical simulation (Figure 2(d)–(f)). Thus, the VCD spectra manifested new chiral aspects upon coordination with Cu(II).

Theoretical analyses of measured VCD spectra: The observed VCD spectra were analysed via DFT calculations, as shown in Figure 2(d)–(f). The details of the structural transformation of a ligand upon coordination were examined. The structure of an isolated [Cu(*SS*-oxa)$(H_2O)_2$](TFMS)$_2$ molecule was theoretically calculated as a model species in solution. Two anions and two H_2O molecules were placed around the Cu(II) ion initially, and the optimised structure is shown in Figure 3(a). In the simulated structure, both phenyl groups in *SS*-oxa were oriented downwards. An oxygen atom in the SO_3 of TFMS$^-$ and a hydrogen atom in the coordinated H_2O formed a hydrogen bond, as their distance was estimated to be 0.16 nm. The results calculated for other models without water molecules, such as [Cu(*SS*-oxa)]$^{2+}$, [Cu(*SS*-oxa)](TFMS)$^+$, and [Cu(*SS*-oxa)](TFMS)$_2$, are provided in the $ESI^†$.

Figure 2(d) shows the VCD and IR spectra of [Cu(*SS*-oxa)$(H_2O)_2$](TFMS)$_2$ calculated for the optimised structure shown in Figure 3(a). The calculated spectra reproduced the observed spectra rather well (Figure 2(a)). Each peak corresponds to the same number in the experimental and theoretical spectra. The results supported the validity of the simulated structure for the complex in solution, and the detailed assignments are provided in the $ESI^†$.

The structure of [Cu(*SS*-oxa)(bzac)](TFMS) was calculated as a model in solution. In the model, bzac$^-$ was assumed to be chelated to the cis-sites of Cu(II), and the optimised structure is shown in Figure 3(b). It should be noted that two molecular

planes were present in the coordinated bzac$^-$. One consisted of a phenyl group and the other consisted of a hexagonal coordination ring, as indicated by the shadowed area. Notably, the two planes were twisted clockwise with a dihedral angle of 27.7° (C1-C2-C3-O). As a result, helical chirality with a *P*-configuration was generated in the coordinated bzac$^-$. This twisting was caused by the steric interference between the phenyl groups in bzac$^-$ and *SS*-oxa. The distances between the two oxygen atoms in bzac and the hydrogen atom in the chiral centre of oxa were estimated to be ~0.26 nm. The anion was located on the opposite side of the bzac ligand. A single O in SO_3 was located in the vicinity of the chiral centre of the oxa ligand with a distance of ~0.24 nm.

Figure 2(e) shows the IR and VCD spectra of [Cu(*SS*-oxa)(bzac)](TFMS) calculated for the corresponding optimised structure in Figure 3(b). The calculated spectra reproduced the observed spectra (Figure 2(b)). The peak at 1425 cm^{-1} (indicated as **c**) was assigned to the asymmetric stretching vibration of C=O bond in bzac$^-$. The appearance of the VCD peak supported the acquisition of structural chirality upon the coordination of bzac$^-$. The other main VCD peaks were assigned as presented in the Supporting Information (ESI$^+$). The calculated VCD and IR spectra of [Cu(*SS*-oxa)(bzac)]$^+$ without an anion are shown in the supporting information(ESI$^+$).

Figure 3(c) shows the optimised structure of [Cu(*SS*-oxa)(dbm)](TFMS). In the coordinated dbm, three molecular planes or two phenyl groups and a coordination hexagon were present, as indicated by **I**, **II**, and **III**. These planes were twisted clockwise in a *P*-configuration (C1-C2-C3-O) with the dihedral angles of 27.5° (for **I/II**) and 24.7° (for **II/III**), respectively. Thus, the dbm$^-$ ligand also acquired a chiral structure upon coordination. Twisting was caused by the steric interference between the phenyl groups in dbm$^-$ and *SS*-oxa. The distances between the two oxygen atoms in dbm and the hydrogen atom at the chiral centre of oxa were estimated to be ~0.26 nm.

Figure 2(f) shows the IR and VCD spectra of [Cu(*SS*-oxa)(dbm)](TFMS) calculated for the optimised structure in Figure 3(c). The calculated IR and VCD spectra reproduced the observed spectra (Figure 2(c)). The peak at 1424 cm^{-1} (indicated as **c**) was assigned to the stretching vibration of the asymmetric C=O stretching in dbm$^-$. The additional peaks (indicated as **a** and **b**) were also predicted at 1582 and 1526 cm^{-1}, respectively. These were assigned to the symmetric C=O stretching or C-C-C stretching of dbm$^-$, respectively. The peak (**d**) at 1338 cm^{-1} was assigned to the C-H bending of dbm$^-$. These peaks assisted the acquisition of the chiral structure by the coordination of dbm$^-$.

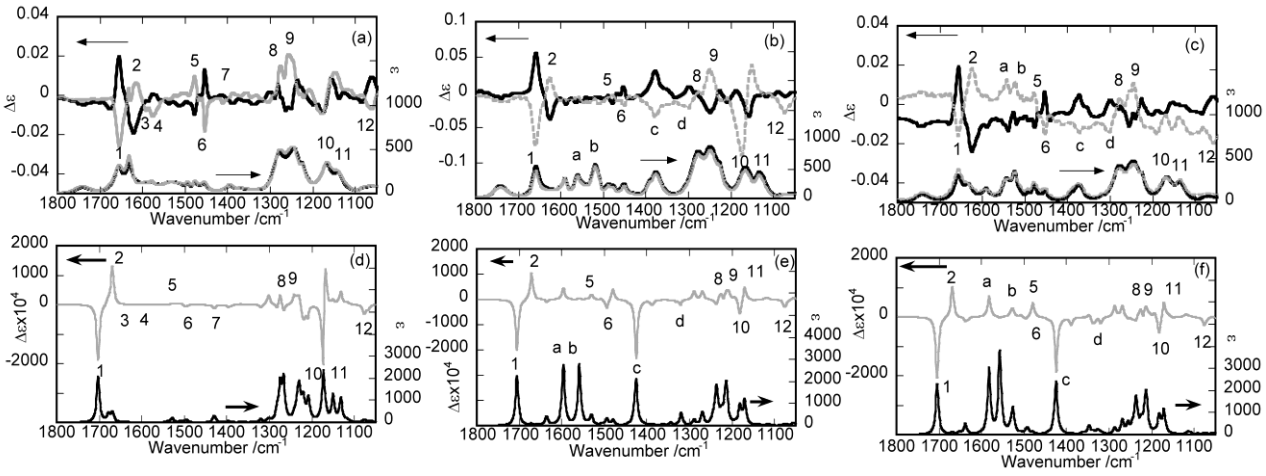

Figure 2. Experimental IR (lower) and VCD (upper) spectra of the $CDCl_3$ solutions of (a) [Cu(*RR*- or *SS*-oxa)](TFMS)$_2$ in $CDCl_3$; (b) [Cu(*RR*- or *SS*-oxa)(bzac)](TFMS) in $CDCl_3$; (c) [Cu(*RR*- or *SS*-oxa)(dbm)](TFMS) in $CDCl_3$. (black) *RR*-oxa and (grey) *SS* -oxa, respectively. In (b) and (c), new peaks are indicated alphabetically.

(d) Calculated IR (lower) and VCD (upper) spectra of [Cu(*SS*- oxa)(H_2O)$_2$](TFMS)$_2$, (e) [Cu(*SS*-oxa)(bzac)](TFMS), (f) [Cu(*SS*-oxa)(dbm)](TFMS). The models of these complexes in $CHCl_3$, using the PCM model. The number and alphabetical delineation of each peak correspond to that of the observed one.

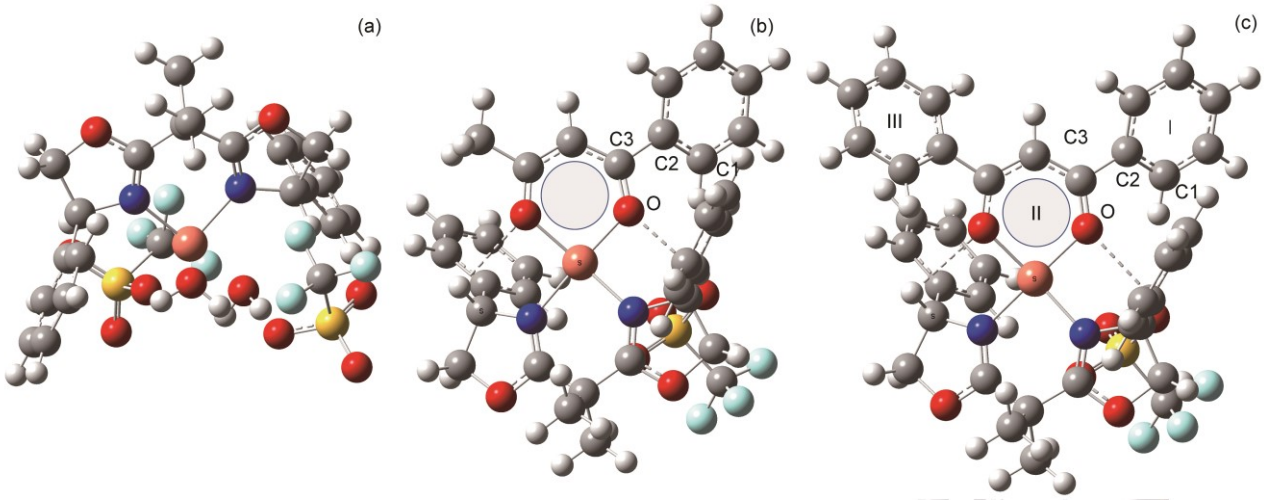

Figure 3. Optimized structures of (a) [Cu(*SS*- oxa)$(H_2O)_2$](TFMS)$_2$; (b) [Cu(*SS*-oxa)(bzac)](TFMS); and (c) [Cu(*SS*-oxa)(dbm)](TFMS).

The source of enantioselectivity during catalysis: Previously, the molecular structure of [Cu(*SS*-oxa)(H_2O)](TFMS)$_2$ was determined via single-crystal X-ray analyses.[2] In the structure, two phenyl groups were oriented in opposite directions. Based on this, an intermediate molecule, [Cu(*SS*-oxa)***S***]$^{2+}$ (***S*** = 3-(*E*)-2-butenoyl-2-oxazolidinone; Chart 1(e)), was constructed theoretically via molecular dynamics simulation, in which ***S*** was coordinated at the cis-vacant sites of [Cu(*SS*-oxa)]$^{2+}$. Here, ***S*** was a substrate for the Michael addition reaction.[2] A marked difference was observed in the steric environment between the upper and lower sides of the double bond in ***S***. Therefore, it was claimed that the enantioselectivity of an addition product was determined by the selection of the two sides. However, a question remains as to whether the structure in a crystalline state reflected that in solutions.

Herein, the structure of [Cu(*SS*-oxa)**L**](TFMS) in solutions was simulated. In the obtained structure, the two phenyl groups were oriented in the same direction (Figure 3(b) and (c)). The coordination around Cu(II) adopted a distorted square geometry. Remarkably, the coordinated ligand transformed to a chiral structure under steric control by the oxa ligand. For the coordinated bzac$^-$ and dbm$^-$ ligands, a twisted chiral conformation was adopted due to the steric interference with the oxa ligand.

These situations indicate the possibility that, during the course of Michael additions, the chirality acquisition in the coordinated state could be the first step in selecting the chirality of the final product. This postulate is based on a view that a reaction intermediate forms a ring structure when a diene adds onto the double bond of a substrate. Examinations of whether the same chiral transformation occurs for a neutral substrate are currently underway.

Experimental Section

Materials: *R*,*R*- and *S*,*S*-2,2'-(dimethylmethylene)bis(4-phenyl-2-oxazoline) (denoted as *R*,*R*-oxa and *S*,*S*-oxa, respectively), copper(II)trifluoromethanesulfonate (denoted as [Cu(TFMS)$_2$]), 1-phenyl-1,3-butanedione (denoted as bzacH), and dibenzoylmethane (denoted as dbmH) were purchased from Tokyo Kasei Co. Ltd. (Japan) and used as received. The preparation of the Cu(II) complexes is described in the Results and Discussion section. All other materials were of reagent grade and used as-purchased. The identification of prepared Cu(II) complexes was performed via HPLC and high-resolution mass spectra (HRMS) as given in the supporting information (ESI$^+$).

Instruments: UV-visible electronic spectra were recorded using a UV–vis spectrophotometer (U-2810, Hitachi Ltd., Japan). ECD spectra were measured using a polarimeter (J-720, JASCO Corporation, Japan). HPLC was performed using a Gulliver HPLC system (JASCO, Japan) with a CAPCELL PAK C_{18} UG column (SHISEIDO, Japan). Electrospray ionisation (ESI) mass spectrometry was performed using an Exactive Plus (Thermo Fisher Scientific) spectrometer with a mass range of *m/z* 20–2000 with a nominal resolution (at *m/z* 200) of 140,000.

VCD measurements: VCD spectra were measured using a machine developed in house with the cooperation of JASCO Corporation, Japan (PRESTO-S-2016 VCD/LD spectrometer). The machine was a concurrent system combined with linear dichroism (LD) and a single PEM system. For measuring a $CDCl_3$ sample, a cell with an optical length of 50 μm was used. The data were accumulated by scanning 10000 times. The baseline correction was performed for the IR and VCD spectra by subtracting the solvent contribution.

Computational details: The IR and VCD spectra of the complexes were theoretically calculated using the Gaussian 16 program(C.01).[30] Geometry optimisation was performed at the DFT level (B3LYP functional with Stuttgart ECP for Cu(II) and 6-31G(d,p) for the other atoms). The PCM model accounted for the solvent effect ($CHCl_3$). The anion (TFMS$^-$) was also

considered for structural optimisation. The VCD intensities were determined from the vibrational rotational strength and the magnetic dipole moments, which were calculated using the magnetic field perturbation theory formulated using magnetic field gauge-invariant atomic orbitals. The calculated intensities were converted to Lorentzian bands with a half-width of 4 cm^{-1} half-width at half-height. The observed spectra were assigned based on the animations of the molecular vibration with Gaussview 6.0 (Gaussian Inc.).

Conclusions

VCD spectroscopy was applied to examine the source of chiral discrimination during asymmetric catalysis. Chiral bis(oxazoline)copper(II) complexes and achiral cationic model ligands (i.e. 1-phenyl-1, 3-butanedione, and dibenzoylmethane) were selected as model reaction intermediates. From the VCD spectra, the coordinated β-diketonato ligands were shown to acquire the chiral character within the coordination sphere. It should be emphasized here that the chiral character induced in a ligand was transient, since it disappeared in a free state. Based on the present findings, it was postulated that the chiral transformation in a coordinated substrate represents the first enantioselective step using the catalyst. Subsequent experiments will be directed toward heterogeneous asymmetric catalysis on a solid support such as clay minerals.

Conflicts of interest

There are no conflicts of interest to declare.

Acknowledgements

This work was financially supported by the JSPS KAKENHI Grant-in-Aid for Scientific Research (B) (JP17H03044) and Scientific Research (C) (JP19K05508) and JST MIRAI grants (JPMJMI18GC). The computations were performed in collaboration with the Research Center for Computational Science, Okazaki, Japan.

Notes and references

1. H. Brunner, *Angew. Chem. Int. Ed.,* 1999, **38**, 1194.
2. J. S. Johnson and D. A. Evans, *Acc. Chem. Res.*, 2000, **33**, 325; D. A. Evans, S. J. Miller, T. Lectka, and P. von Matt., *J. Am. Chem. Soc.*, 1999, **121**, 7559; D. A. Evans, J. S. Johnson*, and* E. J. Olhava, *J. Am. Chem. Soc.*, 2000, **122**, 1635; D. A. Evans, T. Rovis, M. C. Kozlowski, C. W. Downey, and J. S. Tedrow, *J. Am. Chem. Soc.*, 2000, **122**, 9134; D. A. Evans, K. A. Scheidt, J. N. Johnston*,* and M. C. Willis*, J. Am. Chem. Soc.*, 2001, **123**, 4480; D. A. Evans, D. Seidel, M. Rueping, H. W. Lam, J. T. Shaw and C. W. Downey, *J. Am. Chem. Soc.*, 2003, **125**, 12692.
3. E. B. Bauer, *Chem. Soc. Rev.,* 2012, **41**, 3153.
4. R. Brimioulle, D. Lenhart, M. M. Maturi, and T. Bach, *Angew. Chem. Int. Ed.,* 2015, **54**, 3872.
5. T. Cruchter and V. A. Larionv, *Coord. Chem. Soc.*, 2018, **376**, 95.
6. T. Horibe and K. Ishihara, *Chem. Lett.,* 2020, **49**, 107; A. Sakakura, R. Kondo, Y. Matsumura, M. Akakura, and K. Ishihara, *J. Am. Chem. Soc.*, 2009, **131**, 17762.
7. P. S. Steinlandt, W. Zuo, K. Harms, and E. Meggers, *Chem. Eur. J.*, 2019, **25**, 15333.
8. J. M. Fraile, J. I. García, and J. A. Mayoral, *Chem. Rev.*, 2009, **109**, 360; J. M. Fraile, J. I. García, C. I. Herrerías, J. A. Mayoral, and E. Pires, *Chem. Soc. Rev.*, 2009, **38**. 695; J. M. Fraile, J. I. García, C. I. Herrerías, J. A. Mayoral, O. Reiser, A. Socuéllamos, and H. Werner, *Chem. Eur. J.*, 2004, **10,** 2997; J. M. Fraile. J. I. García, J. A. Mayoral, and M. Roldán, *Org. Lett.*, 2007, **9**, 731; J. M. Fraile, N. García, and C. I. Herrerías, *ACS Cat.,* 2013, **3**, 2710.
9. I. P. Beletskaya, C. Nájera, and M. Yus, *Chem. Rev.,* 2018, **118**, 5080.
10. J. Lee, S. Wang, M. Callahan, and P. Nagorny, *Org. Lett.*, 2018. **20**, 2067.
11. W.-T. Hu, X.-Y. Li, W.-T. Gui, J.-Y. Yu, W. Wen, and Q.-X. Guo, *Org. Lett.*, 2019, **21,** 10090.
12. J.-B. Chen, M. Xu, J.-Q. Zhang, B.-B. Sun, J.-M, Hu, J.-Q. Yu, X.-W. Wang, Y. Xia, and Z. Wang, *ACS Catal.*, 2020, **10**, 3556.
13. D. A. Evans, K. A. Woerpel, M. M. Hinman, and M. M. Faul, *J. Am. Chem. Soc.,* 1991, **113**, 726.
14. E. J. Corey, N. Imai, and H. Y. Zhang, *J. Am. Chem. Soc.,* 1991, **113**, 728.
15. G. Desimoni, G. Faita, and K. Jørgensen, *Chem. Rev.*, 2011, **111**, PR284; G. Desimoni, G. Faita, and K. Jørgensen, *Chem. Rev.*, 2006, **106**, 3561.
16. H. Sato, *Phys. Chem. Chem. Phys.,* 2020*,* **22***,* 7671.
17. H. Sato, Y. Mori, and A. Yamagishi, *Dalton Trans.*, 2013, **42**, 6873; H. Sato, K. Takimoto, H. Mori, and A. Yamagishi, *Phys. Chem. Chem. Phys.*, 2018, **20**, 25421.
18. T. M. Keiderling, *Chem. Rev*., 2020, **120**, 3328.
19. L. A. Nafie, *Chirality*, 2020, **32**, 667.
20. C. Merten, *Phys. Chem. Phys. Chem.*, 2017, **19**, 18803; C. Merten, C. H. Pollok, S. Liao, and B. List, *Angew. Chem. Int. Ed.,* 2015, **54**, 8841; T. P. Golub and C. Merten, *Chem. Eur. J.*, 2020, **26**, 2349; C. Merten, *Eur, J. Org. Chem.* 2020, doi: 10.1002/ejoc.202000876.
21. Z. Dezhahang, M. R. Poopari, F. E. Hernández, C. Diaz, and Y. Xu, *Phys. Chem. Phys. Chem.*, 2014, **16**, 12959; C. Merten, K. Hiller, and Y. Xu, *Phys. Chem. Phys. Chem.*, 2012, **14**, 12884.
22. C. Blons, M. S. T. Morin, T. E. Schmid, T. Vives, S. Colombel-Rouen, O. Baslé, T. Reynaldo, C. L. Covington, S. Halbert, S. N. Cuskelly, P. V. Bernhardt, C. M. Williams, J. Crassous, P. L. Polavarapu, C. Crévisy, H. Gérard, and M. Mauduit, *Chem. Eur. J.*, 2017, **23**, 7515.
23. A-C. Chamayou, G. Makhloufi, L. A. Nafie, C. Janiak, and S. Lüdeke, *Inorg. Chem.*, 2015, **54**, 2193.
24. H. Miyake, K. Terada, and H. Tsukube, *Chirality*, 2014, **26**, 293.
25. T. Wu, X.-Z. You, and P. Bouř, *Coord. Chem. Rev.*, 2015, **284**, 1.
26. G. Mazzeo, M. Fusè, G. Longhi, I. Rimoldi, E. Cesarotti, A. Crispini, and S. Abbate, *Dalton Trans.*, 2016, **45**, 992; E. Castiglioni, P. Biscarini, and S. Abbate, *Chirality*, 2009, **21**, E28.
27. J. Sadlej, J. Cz. Dobrowolski, and J. E. Rode, *Chem. Soc. Rev*., 2010, **39**, 1478.
28. S. Abbate, G. Longhi, G. Mazzeo, C. Villani, S. Petković, and R. Ruzziconi*, RSC. Adv.*, 2019, **8**, 11781.
29. K. Naka, H. Sato, T. Fujita, N. Iyi, and A. Yamagishi *J. Phys. Chem. B,* 2003, **107**, 8469.
30. M. J. Frisch et al., *Gaussian 16 (Revision C.01)*, Gaussian, Inc. Wallingford, CT, **2019**.

VCD method was applied for asymmetric catalysis by chiral Cu(II) complexes. When 1-phenyl-1,3-butanedionato was coordinated as a model substrate, it was revealed to be transformed to a twisted chiral form under the steric control by the coordination sphere.

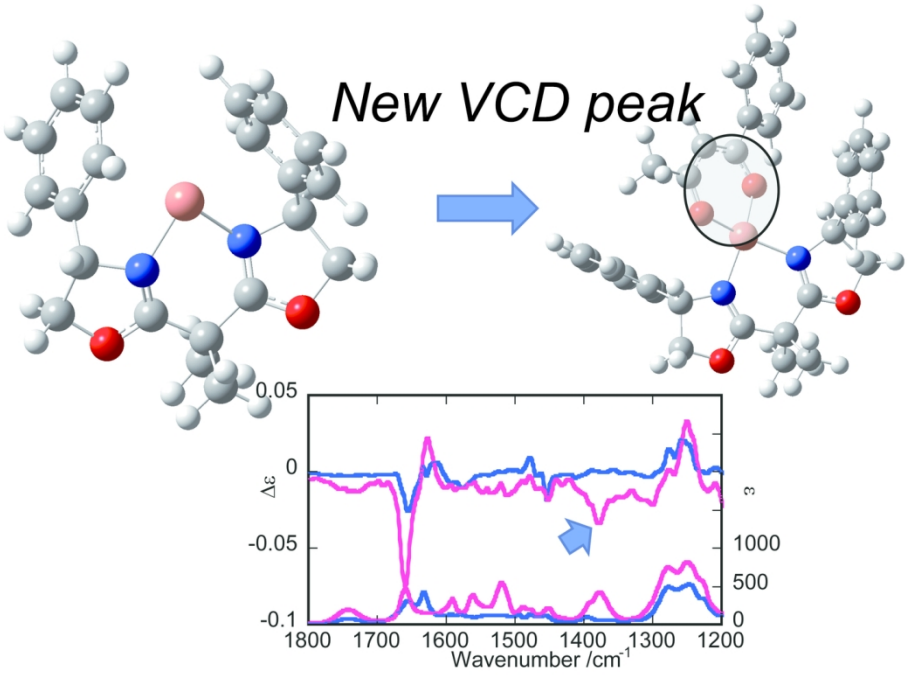

135x93mm (300 x 300 DPI)